Evolution of the Reaction Mechanism during Ultrafast Photoinduced Electron Transfer

Michael G. Kuzmin,* Irina V. Soboleva, and Elena V. Dolotova

Department of Chemistry, Moscow State Lomonosov University, Moscow, 119992 Russia

Received: January 17, 2008; Revised Manuscript Received: March 18, 2008

Specific features of ultrafast photoinduced electron transfer (ET) in concentrated liquid solutions and in neat electron donating solvents are discussed in terms of continuous distribution of ET rate constants, related to electron tunneling with statistical distribution of electronic coupling matrix element and distances between reactant molecules. Available data on photoinduced electron transfer in solutions for several systems are analyzed. Electron tunneling approach is shown to provide global description of nonexponential kinetics of excited states decay at various concentrations of reactant and in neat solvents.

Introduction

Recent progress in experimental investigations of ultrafast photoinduced electron transfer and in molecular-dynamics simulation of donor−acceptor interactions in solution gave the contribution to comprehension of ET features.[1–5] Ultrafast reactions are studied usually in solutions with high quencher concentration or even in neat quencher solvent to avoid translational diffusion control. Under these conditions, significant complications of ET kinetics arise. These complications originate from the inhomogeneity of the environment and reveal some important peculiarities of ET reactions and of solution dynamics. Ultrafast photoinduced ET kinetics in neat electron donating solvents has been discussed earlier using either an electronic coupling matrix element as a dynamic variable,[1] fluctuations of electronic coupling matrix elements,[4,5] or distribution of distinct molecular arrangements with different apparent rate constants.[2] Recently kinetics of ET in such systems was discussed in terms of nonstationary diffusion with constant effective quenching radius.[6]

In this work we try to apply a quite different approach to photoinduced ET kinetics in concentrated liquid solutions and in neat solvents. Kinetics of ET is considered in terms of some probability distribution of ET rate constants related to electron tunneling in the absence of the diffusion in the vicinity of excited molecules. The reaction front propagates extensively from the excited molecule according to the spatial (or temporal) dependence of the rate constant. The distribution of ET rate constants $P(k_{ET})$ is related to the distribution of electronic coupling matrix element, V_{AD}, which exponentially depends on the distance between reactant molecules.[1,4,5,7–10] The diffusion control starts at longer distances when diffusion is faster than the propagation of the reaction front. This approach was used earlier for photoinduced ET in rigid frozen solutions[8–10] and for energy transfer by exchange mechanism.[11] Present work demonstrates that the distribution of ET rate constants provides a good unified description of kinetics of photoinduced ET in the perylene−tetracyanoethylene (PeH−TCNE) system in acetonitrile. This reaction proceeds by an electron tunneling mechanism during the first 10−50 ps consuming molecules of reagents located closer than 1.2−1.5 nm. After that reaction starts to be diffusion controlled. About 0.3−0.8 of PeH* reacts by electron tunneling mechanism at a TCNE concentration 0.1−0.9 M. It is also shown that the distribution approach of rate constants is applicable for the description of the photoelectron transfer in the systems, where solvent acts as an electron donor.

TABLE 1: Kinetic Parameters of PeH* Fluorescence Decay at Various Concentrations of TCNE in MeCN Solution[3]

[TCNE]/M	A_1	τ_1/ps	A_2	τ_2/ps	A_3	τ_3/ps
0.02	0.96	1910	0.04	112		
0.08	0.7	395	0.18	98	0.12	13
0.16	0.46	227	0.29	94	0.25	10.6
0.32	0.35	110	0.35	31	0.3	4.0
0.64	0.23	47	0.33	13.5	0.44	2.9
0.90	0.18	20	0.74	3.67	0.08	0.33

TABLE 2: Kinetic Parameters of PeX* Fluorescence Decay in Neat DMA[2]

PeX	A_1	τ_1/ps	A_2	τ_2/ps	A_3	τ_3/ps
PeH	0.11	13.3	0.66	4.9	0.23	0.87
PeCN	0.01	2.5	0.13	0.97	0.86	0.30
$PeCH_2OH$	0.24	12.0	0.56	5.4	0.20	1.0
$PeCH_3$	0.68	11.4	0.32	4.7		

Experimental Section

Data on kinetics of excited PeH decay in acetonitrile (MeCN) in the presence of various concentrations of TCNE (the free energy of electron transfer $\Delta G^*_{ET} = E(D^+/D) - E(A/A^-) - E_{0,0} = -2.2$ eV) are taken from ref 3 (Table 1). Contribution of Coulombic interaction into ΔG^*_{ET} in MeCN does not exceed 0.1 eV at $r_{AD} > 0.4$ nm. Experimental data on kinetics of excited perylene derivatives (PeX) decay in neat *N*,*N*-dimethylaniline (DMA) are taken from ref 2 and are presented in Table 2. Experimental data on kinetics of excited 7-amino-4-(trifluoromethyl)coumarin (Coumarin 151), and 7-(dimethylamino)-4-(trifluoromethyl)coumarin (Coumarin 152) decay in electron-donating solvents (DMA, *N*,*N*-dimethyl-*o*-toluidine (DMOT), *N*,*N*-dimethyl-*m*-toluidine (DMMT), *N*,*N*,3,5-tetramethylaniline (TMA), *N*,*N*-dimethyl-*p*-toluidine (DMPT), and *o*-anisidine) are taken from ref 1 (Table 3). All of these kinetics were presented by authors as a sum of several exponents $\sum_i A_i \exp(-t/\tau_i)$ with amplitudes A_i and lifetimes τ_i. Original experimental data relevant to Table 1 were kindly put at our disposal by Prof. E. Vauthey.

A spectrum of the observed decay rate constants covers rather wide range: from diffusion controlled value $1/\tau_i < 0.01$ ps^{-1}

* To whom correspondence should be addressed. E-mail: kuzmin@photo.chem.msu.ru.

10.1021/jp8004794 CCC: $40.75
Published on Web 05/20/2008

TABLE 3: Emission Decay Amplitudes and Lifetimes for Coumarin 152 in Electron-Donating Solvents[1]

solvent	A_1	τ_1/ps	A_2	τ_2/ps	A_3	τ_3/ps
DMA			0.2316	2.49	0.7684	0.44
DMOT	0.3735	15.23	0.3735	4.22	0.2530	1.09
DMMT	0.0225	7.19	0.2026	1.46	0.7749	0.29
TMA	0.0299	4.91	0.0934	1.18	0.8767	0.29
DMPT	0.0039	7.06	0.0768	0.94	0.9193	0.22
o-anisidine			0.3187	3.3	0.6813	0.65

($[Q]/\tau_i \approx k_{Diff} \approx 3 \times 10^{10}$ M^{-1} s^{-1} in MeCN at $T = 300$ K) up to value 3 ps^{-1} inherent to ET inside the first solvent shell.

Discussion

Probability Distribution of ET Rates in Solutions. Nonexponential kinetics of ET reactions was observed earlier in many systems in rigid media.[8–10] Such kinetics was discussed in terms of electron tunneling with definite rate constants distribution related to statistical distribution of the distances between reactant molecules. Strongly exergonic ($\Delta G^*_{ET} < -0.5$ *eV*) ultrafast reactions follow the radiationless transition ET mechanism and their rate constants are known[7,10,12] to depend exponentially on the center-to-center distance, r_{AD}, between reactant molecules as

$$k_{ET} = (4\pi^2/h)F_{FC}V_{AD}{}^2 = \nu \exp(-2r_{AD}/a) \qquad (1)$$

where $\nu = (4\pi^2/h)F_{FC}V_0^2$ is the frequency factor, h is Planck's constant, F_{FC} is the Franck−Condon factor, a is the electronic coupling decay factor, $V_{AD}{}^2 = V_0^2\exp(-2r_{AD}/a)$.[5,12]

Kinetics of the excited probe decay caused by ET can be expressed as

$$I(t) = \int_0^\infty P(k_{ET}) \exp(-k_{ET}t)\, dk_{ET} \qquad (2)$$

where $P(k_{ET})$ is the probability distribution of k_{ET} related to the distribution of $V_{AD}{}^2$ and r_{AD}. Approximated treatment of this kinetics[10] uses very strong distance dependence of k_{ET}. A molecule M* is supposed to be quenched, if at least one quencher molecule Q is located inside the sphere with radius r_{AD}, which expands proportionally to $\ln(\nu t)$ (stepwise approximation). In the case of uniform distribution of quencher molecules[10]

$$P(r_{AD})dr_{AD} = 4\pi 0.6[Q] \times \exp\{-0.6[Q](4/3)\pi r_{AD}{}^3\} r_{AD}{}^2\, dr_{AD} = 7.5[Q] \exp(-2.5[Q]r_{AD}{}^3) r_{AD}{}^2\, dr_{AD} \qquad (3)$$

and

$$P(\ln k_{ET})\, d(\ln k_{ET}) = 7.5[Q](a/2)^3[\ln(\nu/k_{ET})]^2 \times \exp\{-2.5[Q](a/2)^3[\ln(\nu/k_{ET})]^3\} \qquad (4)$$

where [Q] is molar concentration of a quencher. Decay kinetics can be approximated by[10,11]

$$I(t)/I_0 = [M^*]/[M^*]_0 = \exp\{-t/\tau_0 - A[Q](\ln(\nu t))^3\} \qquad (5)$$

where τ_0 is an excited-state lifetime in the absence of a quencher, $A = [\pi a^3 N_A/(6 \times 10^{24})] \approx 0.31a^3$ M^{-1} (a is in nm). Apparent ET rate constant decreases with time (at $\nu t > 20$) as $A[Q][\ln(\nu t)]^3/t$. Variations of parameter a in the range from 0.1 to 0.25 nm and parameter ν in the range from 10^{11} to 10^{19} s^{-1} were observed experimentally in various donor−acceptor systems in glassy matrices at 77 K.[7–9] One should take into account that parameters a and ν in equation 4 are interrelated mathematically and their accurate separation is complicated.

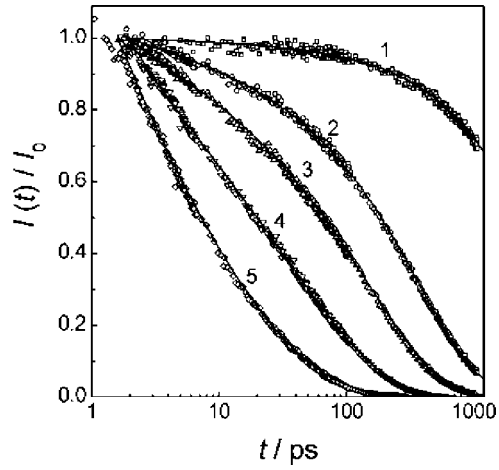

Figure 1. Experimental kinetics of PeH* decay in the presence of various concentrations of TCNE in liquid MeCN (points) and their fitting to eq 6 (lines). [TCNE] = 0.02 (1), 0.08 (2), 0.16 (3), 0.32 (4), 0.64 (5) M.

TABLE 4: Fitting Parameters for PeH*Fluorescence Decay Experimental Data at Various Concentrations of TCNE According to Equation 6[a]

[TCNE]/M	A/M^{-1}	a/nm	$\ln(\nu)$/ps^{-1})	k_Q/M^{-1} ps^{-1}	δt/ps
0.02	0.003	0.21	3.4	0.003	−1.9
	0.002	0.19	3.9	0.015	−1.0
0.08	0.0061	0.27	3.43	0.023	−1.9
	0.005	0.26	3.9	0.027	−1.0
0.16	0.006	0.27	3.61	0.022	−1.9
	0.0055	0.27	3.9	0.024	−0.5
0.32	0.0067	0.28	3.55	0.02	−1.9
	0.0055	0.27	3.9	0.023	−0.5
0.64	0.0087	0.3	3.13	0.013	−1.5
	0.0057	0.27	3.9	0.022	−0.5
0.9	0.007	0.29	3.9	0.03	−0.5

[a] Fitting parameters obtained from the multiexponential approximation (Table 1) are given in every second line (in this case the value of ν was fixed as 50 ps^{-1}).

In liquid solutions we should consider three types of the decay: spontaneous decay with lifetime τ_0, diffusion controlled quenching with monomolecular rate constant $k_Q[Q]$, and electron tunneling inside a sphere where $k_{ET} > k_Q[Q]$. The excited molecule M*, having quencher molecule Q inside this sphere with probability defined by eq 3, reacts predominantly at first. Afterward the reaction is controlled by the diffusion of quencher molecules Q into this sphere. Total time dependence is expressed as

$$I(t)/I_0 = \exp\{-(1/\tau_0 + k_Q[Q])t - A[Q](\ln(\nu t))^3\} \qquad (6)$$

The results of fitting this equation to experimental data on PeH* decay in liquid solutions in MeCN in the presence of various concentrations of TCNE are presented in Figure 1 and Table 4. Some difficulties of fitting are related to the uncertainty of the determination of the initial intensity I_0 (or t_0) in ultrafast measurements.[9] To exclude the uncertainty of t_0, the value ($t + \delta t$) was used in the fitting function as an independent variable, where δt was a variable parameter. Direct experimental values of $I(t)$ were used for fitting as well as values of $I(t)$ recovered from triexponential approximation. Both data gave similar values of parameters A, $a = (A/0.31)^{1/3}$ nm, ν, and k_Q. Table 4 demonstrates that obtained parameters are practically constant

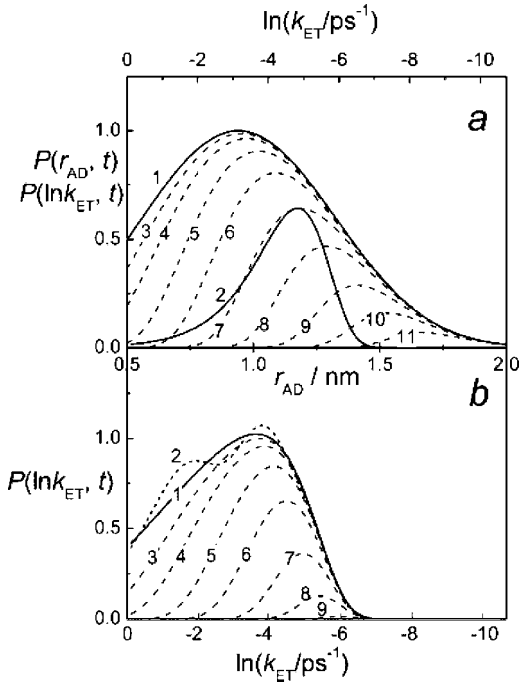

Figure 2. (a) Spatial distribution of TCNE molecules $P(r_{AD})$ and distribution of ET rate constants for electron tunneling $P(\ln k_{ET})$ for PeH*−TCNE in MeCN ([TCNE] = 0.32 M). Solid line 1 corresponds both to the statistical distribution of the distances between PeH and TCNE molecules, $P(r_{AD})$, in accordance with eq 3, and to the distribution of the rate constants, $P(\ln k_{ET})$ in accordance with eq 4 with experimentally obtained parameters (Table 4). Solid line 2 corresponds to the diffusion rates, $P(\ln k_{Diff})$. Dash lines 3−11 demonstrate the evolution of $P(r_{AD})$ with time (1, 3, 10, 30, 100, 300, 1000, 3000, and 10 000 ps, respectively). (b) Distribution of ET rate constants, $P(\ln k_{ET})$, for combined electron tunneling and diffusion quenching in the same system (solid line 1). Dash line 2 corresponds to the original triexponential approximation of experimental data on PeH* fluorescence decay according to eq 8. Dash lines 3−9 show the evolution of $P(\ln k_{ET})$ with time (1, 3, 10, 30, 100, 300, and 1000 ps).

in the range of [Q] from 0.08 to 0.64 M, giving strong evidence for control of ET rates by the intermolecular distance distribution around excited molecules and electron tunneling mechanism of ET. The obtained value of $a \approx 0.28$ nm is close to aforementioned experimental values of Verhoeven[12] and about 2−3 times larger than quantum chemistry estimations.[4,5]

The obtained value of $\nu = (4\pi^2/h)V_0^2F_{FC} \approx 3 \times 10^{13}$ s^{-1} provides $V_0^2F_{FC} \approx 0.003$ eV. Similar value of $V_{AD}^2F_{FC} \approx 0.001$ eV for contact pair of reactants could be evaluated as $V_{AD}^2F_{FC} = (k_0/V_Q)/(4\pi^2/h)$ using the value of maximum (kinetic) rate constant $k_0 = 0.2$ M^{-1} ps^{-1} obtained in ref 6 and a molar volume of a quencher $V_Q = 0.13$ dm^3 mol^{-1}. Franck−Condon factor can be evaluated from the energy gap $\Delta E = -(\Delta G_{ET}^* + \lambda_S)$ between locally excited and charge transfer states as[16]

$$F_{FC} = (1/\sigma\sqrt{2\pi})\sum_m [\exp(-S)S^m/m!] \times \exp[-(\Delta E - mh\nu_v)^2/2\sigma^2] \quad (7)$$

where $h\nu_V$ is the dominant high frequency vibration mode, $S = \lambda_V/h\nu_V$ is the Huang−Rhys spectral factor, $\sigma^2 \approx 0.01-0.02$ eV^2 is a distribution width parameter, and λ_S is the reorganization energy. Variations of these parameters in the range $h\nu_V \approx 0.15-0.2$ eV, $S \approx 1.5-2$, $\sigma^2 \approx 0.01-0.02$ eV^2, and $\lambda_S \approx 0.6-1.0$ eV do not affect essentially the value of $F_{FC} \approx 10^{-3}-10^{-2}$ eV^{-1} for $\Delta E = 2.14$ eV when perylene cation radicals PeH$^{\bullet+}$ are formed in the ground state. In the case that cation radicals PeH$^{\bullet+}$ are formed in the electronically excited state[6] $\Delta E < 0.6$ eV and $F_{FC} \approx 1$ eV^{-1}. Estimated values of V_0 are ca. 1 eV for formation of the ground-state of PeH$^{\bullet+}$ and 0.05 eV for formation of the excited PeH$^{\bullet+}$. As we shall see below V_{AD} for the reactions inside the first solvation shell ($r_{AD} \approx 0.4$ nm) are in the range 0.003 − 0.02 eV. This is close to evaluation of $V_{AD} = V_0 \exp(-r_{AD}/a)$ for $r_{AD} = 0.3-0.6$ nm, $a = 0.28$ nm and $V_0 = 0.05$ eV obtained earlier for less exergonic reaction yielding electronically excited PeH$^{\bullet+}$. This means that the formation of the excited PeH$^{\bullet+}$ turns out to dominate. Evaluated values of V_{AD} in the case of formation of the excited PeH$^{\bullet+}$ are close to the typical values of V_{AD} in contact ground-state CT complexes and exciplexes which vary in the range 0.01−0.5 eV.[13−15] Rates of formation of ground-state or electronically excited-state of radical ions in ET reaction have identical distance dependence on the electronic coupling factor and cannot give any evidence for their distinctions. In contrast, for thermally activated medium reorganization (Marcus) mechanism much smaller rate factor (calculated as $\exp[-(\Delta G_{ET}^* + \lambda_S)/4\lambda_S k_B T]$) is expected for the formation of ground relative to excited-state of PeH$^{\bullet+}$ (10^{-6} and 0.4, respectively).

Figure 2a shows an example of the distributions $P(r_{AD})$ (eq 3) and $P(\ln k_{ET})$ (eq 4) for PeH*/TCNE in MeCN ([TCNE] = 0.32 M) according to the electron tunneling model with parameters obtained from the fitting of direct experimental data on $I(t)$ to eq 6. Since $\ln k_{ET}$ and r_{AD} are linear dependent (eq 1), the distributions $P(r_{AD})$ and $P(\ln k_{ET})$ have the same shape (line 1). Curve 2 corresponds to $P(\ln k_{ET})$ for diffusion quenching rate $k_Q[Q]$. This function has the form $(k_{Diff}/k)\exp(-k_{Diff}/k)$ rather than the form of delta-function because of specific property of the inverse Laplace transform which provides identical $I(t) = \exp(-k_0 t)$ for monoexponential decay with rate constant k_0 and for multiexponential decay with the distribution $P(k) = (k_0/k)\exp(-k_0/k)$.

Figure 2b demonstrates the distribution $P(\ln k_{ET})$ for combined electron tunneling and diffusion quenching in the same system (line 1). Line 2 presents the distribution calculated from the authors' triexponential approximation of $I(t)$ (Table 4) as

$$P(\ln k_{ET}(t)) = -d(\ln I(t))/d(\ln t) = \sum_i A_i(t/\tau_i)\exp(-t/\tau_i) \quad (8)$$

where $k_{ET}(t) = 1/t$.[10] One can see that both curves are close to each other, but the curve corresponding to statistical distribution of a quencher is smoother. In fact the maxima of curve 2 arise when a triexponential approximation of the experimental kinetics is used.

Figure 2 presents also time evolution of the distribution function calculated as $P(r_{AD}, t) = P(r_{AD}, 0)\exp(-tk_{ET})$ (curves 3−11 in Figure 2a) and $P(\ln k_{ET}, t) = P(\ln k_{ET}, 0)\exp(-tk_{ET})$ (curves 3−9 in Figure 2b) according to the consumption of TCNE molecules in the vicinity of excited molecules of PeH* and transformation of distance (or V_{AD}^2) control into diffusion control. One can see that during first 100 ps electron tunneling mechanism dominates and reaction front moves to greater distances between PeH* and TCNE molecules (smaller k_{ET}). Only when $k_Q[Q]$ becomes higher than $k_{ET}(t)$ does quenching become predominantly diffusion controlled, and the slow exponential term $A_1\exp(-t/\tau_1)$ can be attributed to the diffusion controlled quenching.

Diffusion control starts to dominate at the distance R_Q, that can be estimated as $R_Q = (a/2)\ln\{\nu/(k_Q[Q])\}$ from the equality $k_Q[Q] = \nu\exp(-2r_{AD}/a)$. For the reaction between PeH* and

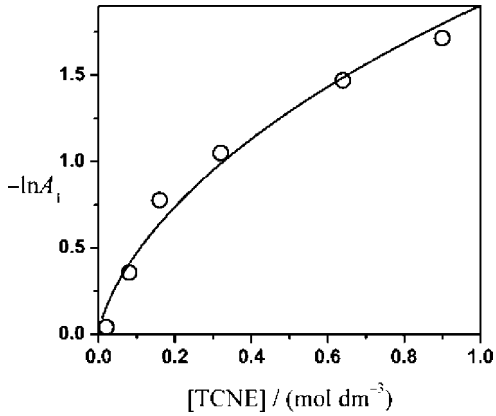

Figure 3. Experimental dependence of the amplitude A_1 of the longest exponential term on TCNE concentration (points) and its simulation, using eq 9.

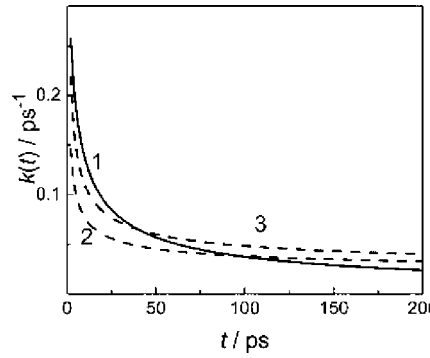

Figure 4. Simulated time dependences of the apparent electron tunnelling rate constant $k_{ET}(t) = \pi a^3 N_A[\ln(\nu t)]^3/t$ (solid line 1, $\nu = 35$ ps^{-1} and $a = 0.28$ nm) and nonstationary diffusion rate constant $k(t) = k_{Diff}(1 + \sqrt{4r_{AD}/k_{Diff}t})$ (dashed lines 2 and 3): $k_{Diff} = 0.02$ ps^{-1} and $r_{AD} = 0.4$ nm (line 2) and $r_{AD} = 1$ nm (line 3).

TCNE $R_Q \approx 0.9-1.4$ nm for [Q] = 0.9−0.02 M and obtained values of a and ν. This distance corresponds to lose pairs of reactants and $t >$ exp $(2R_Q/a)/\nu = 20-900$ ps for various concentrations [Q]. The distance slowly increases with decrease of [Q] and corresponds to the sphere, which has no quencher molecule inside. So large R_Q is consistent with large value of diffusion controlled quenching rate constant $k_Q = 0.02-0.03$ M^{-1} ps^{-1} = (2−3) × 10^{10} M^{-1} s^{-1}, which coincides with that obtained from the slope of the plot $1/\tau_1$ vs [Q].[3] In contrast to ordinary static quenching described by conventional Perrin equation $I/I_0 = \exp(-[4/3]\pi R_Q{}^3 N_A[Q])$ (the part of molecules M, which have no molecules Q inside a sphere with radius R_Q) nonlinear dependence of ln A_1 vs [Q] is observed (Figure 3) because of the concentration dependence of R_Q

$$\ln A_1 = -\frac{4}{3}\pi R_Q{}^3 N_A[Q] = -\frac{4}{3}\pi N_A[Q]\left\{\frac{a}{2}\ln[\nu/(k_Q[Q])]\right\}^3 \quad (9)$$

This expression describes well experimental dependence of A_1 vs [Q] with parameters $a = 0.28$ nm and $\ln(\nu/\text{ps}^{-1}) = 2.6$, which are close to that obtained by fitting of the complete decay kinetics.

Earlier, the kinetics of the reaction between PeH* and TCNE was discussed in terms of the differential encounter theory,[6] which considered the time dependent rate constant $k(t)$ and generally took into account spatial distribution of reactants and nonstationary diffusion. A rather small radius for the diffusion controlled reaction ($R_Q = 0.82$ nm) was obtained for single channel (formation of ground-state PeH$^{\bullet+}$) and double channel (formation of ground and electronically excited states of PeH$^{\bullet+}$) mechanisms using distance dependent $V_{AD}{}^2 = V_0{}^2 \exp[-2(r - r_0)/a]$ with relatively small value of the electronic coupling decay parameter $a = 0.124$ nm and distance dependent reorganization energy $\lambda(r) = \lambda(2 - r_0/r)$ (r_0 is the closest approach distance) and Marcus activation energy $\Delta G^{\ddagger}(r) = [\Delta G_{ET}(r) + \lambda_S(r)]^2/4\lambda_S(r)$. Authors came to the conclusion that the quenching was under diffusion control with $R_Q = 0.82$ nm. In the present approach we obtained significantly slower distance dependence of $V_{AD}{}^2$ ($a = 0.28$ nm) and consequently greater $R_Q = 0.9-1.4$ nm for the radius of the diffusion controlled reaction. On this reason electron tunneling inside the sphere of radius R_Q occurs to be more important and its contribution into the total quenching amounts up to 0.3−0.8 at TCNE concentrations from 0.08 to 0.9 M.

Figure 4 presents simulated time dependences of the apparent $k_{ET}(t) = \pi a^3 N_A[\ln(\nu t)]^3/t$ for the electron tunneling mechanism with obtained earlier values of $\nu = 35$ ps^{-1} and $a = 0.28$ nm and of nonstationary diffusion rate constant $k(t) = k_{Diff}(1 + \sqrt{4r_{AD}/k_{Diff}t})$ with $k_{Diff} = 0.02$ ps^{-1} and $r_{AD} = 0.4$ nm. This figure demonstrates that the electron tunnelling mechanism dominates at $t < 100$ ps according to the previous discussion though both $k_{ET}(t)$ and $k(t)$ increase rapidly with the decrease of t. In order to obtain the time dependence of the nonstationary diffusion rate constant close to the observed one (Figure 4, line 3), one has to use the value of $r_{AD} > 1$ nm. So a large distance means implicitly long-distance electron transfer. Thus, the static (distance distribution) and dynamic approaches (nonstationary diffusion) yield very close time dependent apparent ET rate constant for electron tunnelling.

ET Rates in Neat Electron Donating Solvents. Nonexponential kinetics of ET is observed also in neat electron donating solvents. This kinetics was considered earlier in terms of dynamic variable V_{AD}[1] and in terms of distribution of distinct molecular arrangements with different apparent rate constants.[2] We shall treat this kinetics in terms of probability distribution of k_{ET}.

Strong high frequency fluctuations of electronic coupling matrix element, V_{AD}, from 0.01 to 0.4 eV were found by the combined quantum chemistry and molecular-dynamics calculations[4,5] for oxazine and 9-cyanoanthracene in DMA for molecules located inside the first solvent shell with the average value $V_{AD}{}^2 \approx 0.002$ eV^2.[5] This value exceeds more than 3 orders of magnitude the values of $V_{AD}{}^2$ outside this shell, where it decreases exponentially with the increase of distance between reactant molecules. Variations of $V_{AD}{}^2$ inside the first solvent shell were considered as a result of fluctuations of intermolecular orientation and edge-to-edge distances.[1,4,5] Probability distribution of ET rate constants, $P(\ln k_{ET})$, inside the first solvent shell should be similar to the distribution of $V_{AD}{}^2$.

Experimental data on fluorescence decay kinetics for perylene derivatives in neat DMA (Table 2) were found to be fitted well to exponential function

$$I(t)/I_0 = \exp[-(ct)^b] = \exp[-c^b \exp(b \ln t)] \quad (10)$$

Results of the fitting are shown in Figure 5 and Table 5. Equation 10 corresponds to the distribution function

$$P(\ln k_{ET}) = bc^b \exp(-b \ln k_{ET}) \exp\left[-c^b \exp(-b \ln k_{ET})\right] \quad (11)$$

which has a maximum at $\ln k_{ET}{}^{Max} = -\ln c$ and implies that the distribution relaxation occurs much slower than ET. In contrast,

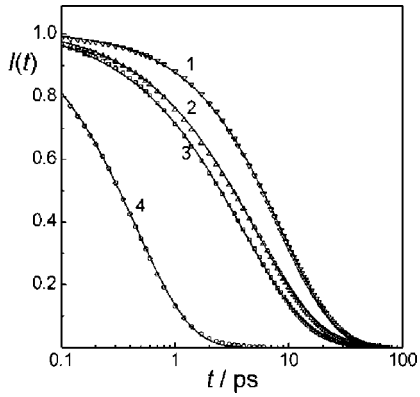

Figure 5. Fitting of eq 10 to experimental kinetics of excited perylene derivatives fluorescence decay in liquid solutions in DMA (points).[2] 1, PeH; 2, PeCN; 3, $PeCH_2OH$; 4, $PeCH_3$.

TABLE 5: Fitting Parameters for Fluorescence Decay of Perylene Derivatives in DMA[2] and Coumarin 151 (C151)[1] and Coumarin 152 (C152)[1] in Various Electron-Donating Solvents According to eq 10

system	b	c/ps^{-1}	ln c	δt/ps	ΔG^*_{ET}/eV (ε = 37.5)
PeH in DMA	0.73	0.26	−1.35	−0.03	−0.44
PeCN in DMA	0.88	2.3	0.83	−0.05	−0.54
$PeCH_2OH$ in DMA	0.75	0.20	−1.61	−0.01	−0.43
$PeCH_3$ in DMA	0.90	0.12	−2.12	−0.05	−0.44
C152 in DMA	0.66	1.82	0.59	−0.03	−0.29
C151 in DMA	0.66	1.3	0.26	0.0	
C152 in DMOT	0.56	0.26	−1.34	−0.3	
C152 in DMMT	0.59	4.35	1.47	−0.05	
C152 in TMA	0.61	5.9	1.77	−0.15	−0.30
C152 in DMPT	0.72	7.1	1.97	−0.22	−0.33
C152 in *o*-anisidine	0.42	5.9	1.77	−0.47	−0.38

ordinary first order decay with approximately constant quenching parameter (contact rate constant k_0)[6,15] is expected in the case when relaxation is faster than ET. Distribution function 11 has the shape similar to the Gaussian distribution function $P(\ln k_{ET}) = (1/\sigma\sqrt{2\pi})\exp\{-0.5[(\ln k_{ET} - \ln k_{ET}^{Max})/\sigma]^2\}$, but can be integrated in the analytical form to obtain fitting function 10. All perylene derivatives, except PeCN, have similar k_{ET}^{Max} (Table 5). A much greater value of $\ln k_{ET}^{Max}$ for PeCN can be attributed to much stronger electronic coupling, caused by some attraction between PeCN and DMA molecules due to oppositely directed dipole moments in the ground-state configuration, corresponding to maximum electronic coupling between electron donor and acceptor.[2]

Castner et al.[1] observed similar polyexponential decay kinetics for two coumarins: Coumarin 151 and Coumarin 152 in various electron-donating solvents with different ΔG^*_{ET}. We found that this kinetics could also be well described by equation 10 (Figure 6) with parameters close to that for PeX in DMA (Table 5) when $\Delta G^*_{ET} < -0.3$ eV. Evaluations of the reorganization energy in the electron-donating solvents used ($\varepsilon_S = 4-6$, $r_{AD} = 0.4$ nm) give the value $\lambda_S \approx 0.3-0.4$ eV. The energy gap is equal to $\Delta E = -(\Delta G^*_{ET} + \lambda_S) > 0$ for these solvents. For other electron-donating solvents (triethylamine, triphenylamine, dimethyl phthalate), when $\Delta G^*_{ET} > -0.2$ eV and $\Delta E < 0$, equation 10 cannot provide reasonable description of the fluorescence decay. Probably for these compounds ET requires some activation energy due to negative ΔE and electron tunneling mechanism fails.

Therefore, a relatively large dispersion of k_{ET} exists even in neat solvents in the absence of diffusion and distance distribution

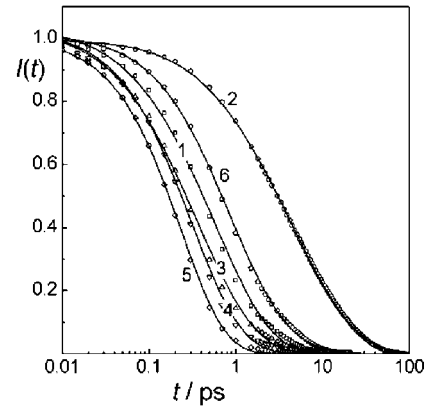

Figure 6. Fitting of eq 10 to experimental kinetics of excited Coumarin 152 fluorescence decay in electron-donating solvents: 1, DMA; 2, DMOT; 3, DMMT; 4, TMA; 5, DMPT; 6, *o*-anisidine.

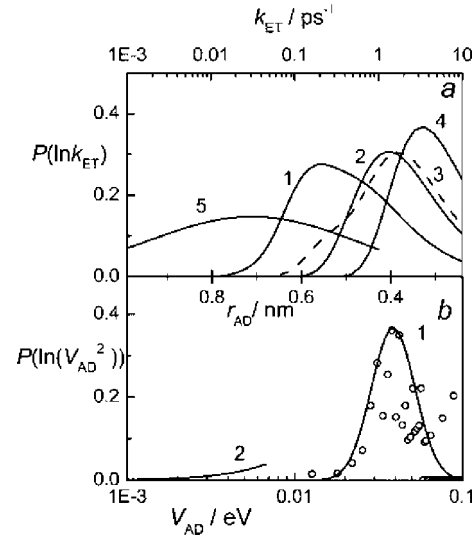

Figure 7. (a) Dependences of the distribution of $P(\ln k_{ET})$ on k_{ET} for the first solvent shell for PeH (1), PeCN (2), coumarin 152 (3), coumarin 151 (4) in neat DMA, and outer solvent shell for PeH*/TCNE in MeCN ([TCNE] = 0.32 M) (5) according to ET kinetics measurements (present work). (b) Dependences of the distribution $P(\ln V_{AD}^2)$ for the first solvent shell (1) and outer solvent shell (2) on electronic coupling V_{AD}, according to quantum chemistry calculations[4,5] for 9-cyanoanthracene/DMA.

of reactant molecules. During the first few ps, ET occurs with $k_{ET} = (4\pi^2/h)F_{FC}V_{AD}^2 \approx 0.1-10$ ps^{-1} (eq 1, where $F_{FC}V_{AD}^2 \approx 10^{-5}-10^{-3}$ eV) and rate constants are controlled by statistical distribution of electronic coupling matrix element V_{AD} (Figure 7b) related to the distribution and fluctuations of mutual orientation and displacements of reactant molecules inside the first solvent shell.

Comparison of experimental data on k_{ET} and results of combined quantum chemistry and molecular dynamics calculations[4,5] of V_{AD}^2 presented in Figure 7, demonstrates qualitative correlation between the experimental rate constants distribution $P(\ln k_{ET})$ and distribution of electronic coupling matrix element $P(\ln V_{AD}^2)$ for both the first solvent shell and outer solvent shells. But quantitative comparison of these data shows essential difference between experimental data and quantum chemistry estimations. It turns out that quantum chemistry calculations provide reasonable values of $\langle V_{AD}^2 \rangle$ for the first solvent shell but overestimate its distance decay outside the first solvent shell. $P(\ln k_{ET})$ for solutions of perylene derivatives and coumarins in neat DMA have a maximum in the range $k_{ET} = 0.1-3$ ps^{-1}

corresponding to $F_{FC}V_{AD}^2 \approx (0.1-3) \times 10^{-4}$ eV in the first solvent shell. The Franck−Condon factor for these systems with $\Delta G_{ET}^* > -0.5$ eV should reach ca. 1 eV^{-1} and $V_{AD}^2 \approx (0.1-3) \times 10^{-4}$ eV^2 is close to calculated distribution of $\langle V_{AD}^2 \rangle = (0.5-3) \times 10^{-3}$ eV^2 for the first solvent shell for oxazine-1 and 9-cyanoanthracene in DMA.[5] But no significant drop of k_{ET} between the first and the second solvent shells is observed experimentally, which indicates rather gradual changes of electronic coupling and other properties in going from the first to outer solvent shell in contrast to quantum chemistry calculations where V_{AD}^2 decreases more than 1000 times when going from the first ($r_{AD} < 0.6$ nm) to the second solvent shell ($r_{AD} > 0.6$ nm). As discussed earlier, values of $V_{AD}^2 = 0.002 \exp(-2r_{AD}/a)$ eV^2 with $a = 0.28$ nm obtained for the reaction of excited perylene with tetracyanoethylene in acetonitrile solutions (yielding excited perylene cation radicals) show a gradual decrease of V_{AD}^2 from 10^{-4} eV^2 at $r_{AD} \approx 0.45$ nm to 10^{-5} eV^2 at $r_{AD} \approx 0.75$ nm. A similar slow decrease of k_{ET} with the distance with $a \approx 0.2$ nm was observed experimentally for through-bond intramolecular ET in rigid organic molecules.[12] For this reason, electron tunneling can compete with the diffusion even at $r_{AD} = 1.0-1.5$ nm.

The essential difference between experimentally observed $a = 0.28$ nm and quantum chemistry estimations[5] of $a = 0.08$ nm can be attributed probably to the intermolecular medium effect. This effect should decrease the energy of an electron between the donor and acceptor molecules and decelerate the decay of V_{AD}^2 with the distance. Some part of the dramatic difference in experimental values of k_{ET} and quantum chemistry calculations of V_{AD}^2 can be attributed also to the contribution of the distance dependence of the Franck−Condon factor into k_{ET}. According to eq 7 F_{FC} is found to decrease significantly at short distances since vertical (Franck−Condon) energy gap between locally excited and charge transfer states for radiationless transition increases at small distances:

$\Delta E = \Delta E_0 + (e^2/4\pi\varepsilon_0)/(n^2 r_{AD})$, where ΔE_0 is ΔE at an infinite distance, n is refraction index of the solvent, e and $4\pi\varepsilon_0$ are the charge of an electron and electric constant ($e^2/4\pi\varepsilon_0 = 1.44$ eV nm). Thus even a decrease of k_{ET} at small r_{AD} (<0.6 nm) is possible as well as weaker distance dependence of k_{ET} as compared to V_{AD}^2 at moderate distances ($0.6 < r_{AD} < 1.0$ nm).

Effect of Franck−Condon factor on rates of electron tunneling was studied in glassy solution at 77 K.[17] The decrease of k_{ET} was observed for endergonic ($\Delta G_{ET}^* > -0.3$ eV) and for strongly exergonic ($\Delta G_{ET}^* < -1.2$ eV) reactions.

In general, nonexponential fluorescence decay can be caused by some other reasons rather than the tunneling mechanism of ET. For instance, nonexponential fluorescence kinetics of fluorescent probes containing complexes of Ru^{2+} in solutions of water soluble polymers[18] was attributed to some local inhomogeneities in the polymer backbone. Even rigid polymers contain microinhomogeneous regions with high mobility of small molecules.[19] In this aspect common liquid solutions provide the best example of homogeneous system with statistical distribution of reactant molecules.

Conclusion

Analysis of kinetics in terms of probability distribution of rate constants allows to show spectacularly the evolution of mechanism of ultrafast ET. Consecutive transformations of crucial factors, which control the reaction mechanism and the reaction rate, occur during the first 1−50 ps after photoexcitation. Conditions of these transformations can be estimated from the concentration dependence of the parameters describing the kinetics of ET. Ultrafast ET kinetics provides a possibility to recover electron tunneling parameters (ν, a, and F_{FC}) in solutions and the features of electronic coupling distribution in neat solvents. It should be particularly emphasized that kinetics of less exergonic ET (when $\Delta G_{ET}^* > -\lambda_S$) can not be described in the frame of electron tunneling approach, because such reactions have an activation barrier and proceed much slower.

In the first few ps, the reaction rate is controlled by statistical distribution of electronic coupling matrix element V_{AD} (described by Gauss function or by eq 11), related to the fluctuations of mutual orientation and displacements of reactant molecules inside the first solvent shell.

During the subsequent 10−50 ps, ET follows the electron tunneling mechanism and the front of the reaction expands with the rate exponentially decreasing with the distance and time, according to the spatial distribution of quencher molecules outside the first solvent shell (eqs 3 and 4). Here V_{AD} varies according to the distance between the reactant molecules. In the case of uniform distribution of quencher molecules in the solution the distribution $P(\ln k_{ET})$ is described by the eq 4. When ET rate decreases below the rate of diffusion ($k_{ET} < k_{Diff}[Q]$) the reaction becomes ordinary diffusion controlled reaction (after 10−50 ps and $r_{AD} > 1-2$ nm, depending on a quencher concentration). Common term "static quenching" can be attributed not only to the ground-state complex formation but also to ultrafast ET inside the first and the second solvent shells around excited molecule.

Comparison of experimental data and results of combined quantum chemistry and molecular dynamics calculations[4,5] demonstrates qualitative correlation between the experimental rate constants distribution $P(\ln k_{ET})$ and quantum chemical calculations of $P(\ln V_{AD}^2)$. However, the essential quantitative difference between experimental data and quantum mechanical calculations was found for a distance dependence of k_{ET} and V_{AD}^2. No significant drop of k_{ET} between the first and the second solvent shells is observed experimentally in contrast to quantum mechanical calculations.[5] This indicates more gradual changes of electronic coupling and other properties in going from the first to outer solvent shell. Similar contradictions between experimental data and quantum chemistry calculations are observed for contact CT complexes and exciplexes. Calculated values of $V_{AD}^2 = 0.002$ eV^2 for the first solvent shell for oxazine-1 and 9-cyanoanthracene in DMA[5] are ca. 10−50 times smaller than the values $V_{AD}^2 = 0.02-0.1$ eV^2 obtained from spectral data for exciplexes and contact CT complexes.[13−15]

The analyzed approaches of probability distribution of rate constants and of time-dependent (non-Markovian) rate constants are similar to each other to some extent because they are related to the same function $I(t)$. However, the distribution function $P(\ln k_{ET})$ reflects more distinctly and directly the physical behavior of the phenomenon (for instance, distance and mutual orientation of reactants molecules). The use of the distribution function $P(\ln k_{ET})$ is similar to the use of Maxwell−Boltzmann distribution and distortions from this distribution in the process of fast reactions in ordinary chemical kinetics.

Nonexponential fluorescence decay in viscous solutions was discussed in terms of long-range ET and distribution of electron transfer distances in liquid and solid solutions by Tachiya et al.[20,21] However, in contrast to the analytical approximation used in the present work, the authors used less convenient simulation procedure to extract electron tunneling parameters from the experimental fluorescence decay kinetics.

Thus, a transformation of ET mechanism during first 10−50 ps causes temporal and spatial differentiating among radical ion

pairs and complicates significantly the kinetics of ET reactions. All of these effects can be used for creation of nanostructures and for control of electron transport in organized molecular systems. The approach, proposed in this work, allows us to present more clearly the evolution of the physical nature of the factors, controlling the reaction rate in contrast to traditional one.

Acknowledgment. This work was supported by Russian Foundation for Basic Researh, Project Nos. 05-03-32554 and 07-02-91016. Authors express gratitude to Prof. Eric Vauthey for the provided experimental data.

References and Notes

(1) Castner, E. W.; Kennedy, D.; Cave, R. J. *J. Phys. Chem. A* **2000**, *104* (13), 2869.
(2) Morandeira, A.; Fürstenberg, A.; Gumy, J.-C.; Vauthey, E. *J. Phys. Chem. A* **2003**, *107* (28), 5375.
(3) Pagès, S.; Lang, B.; Vauthey, E. *J. Phys. Chem. A* **2004**, *108* (4), 549.
(4) Scherer, P. O. J. *J. Phys. Chem. A* **2000**, *104* (26), 6301.
(5) Scherer, P. O. J.; Tachiya, M. *J. Chem. Phys.* **2003**, *118* (9), 4149.
(6) Gladkikh, V.; Burstein, A. I.; Angulo, G.; Pagès, S.; Lang, B.; Vauthey, E. *J. Phys. Chem. A* **2004**, *108* (32), 6667.
(7) Bell, R. P. *The Tunnel Effect in Chemistry*; Chapman and Hall: New York, 1980.
(8) Khairutdinov, R. F.; Sadovskii, N. A.; Parmon, V. N.; Kuzmin, M. G.; Zamaraev, K. I. *Acad. Nauk SSSR. Proc. Phys. Chem. Sect.* **1975**, *220*, 104.
(9) Sadovskii, N. A.; Kuzmin, M. G. *Acad. Nauk SSSR. Proc. Phys. Chem. Sect.* **1975**, *222*, 643.
(10) Khairutdinov, R. F.; Zamaraev, K. I.; Zhdanov, V. P. *Comprehensive Chem. Kinet.* **1989**, *30*, 359.
(11) Inokuti, M.; Hirayama, F. *J. Chem. Phys.* **1965**, *43*, 1978.
(12) Verhoeven, J. W. *Adv. Chem. Phys.* **1999**, *106*, 603.
(13) Gould, I. R.; Yong, R. H.; Mueller, L. J.; Farid, S. *J. Am. Chem. Soc.* **1994**, *116* (18), 8176.
(14) Gould, I. R.; Yong, R. H.; Mueller, L. J.; Albrecht, A. C.; Farid, S. *J. Am. Chem. Soc.* **1994**, *116* (16), 8188.
(15) Kuzmin, M. G.; Dolotova, E. V.; Soboleva, I. V. *Russ. J. Phys. Chem.* **2002**, *76*, 1109.
(16) Ulstrup, J.; Jortner, J. *J. Chem. Phys.* **1975**, *63*, 4358.
(17) Miller, J. R.; Beitz, J. V.; Huddleston, R. K. *J. Am. Chem. Soc.* **1984**, *106* (18), 5057.
(18) Laguitton-Pasquier, H.; Martre, A.; Deronzier, A. *J. Phys. Chem. B* **2001**, *105* (21), 4801.
(19) Kalechitz, I. I.; Zubov, V. P.; Kabanov, V. A.; Kuzmin, M. G. *High Mol. Compnd.* **1984**, *26* (A), 576.
(20) Murata, S.; Tachiya, M. *J. Phys. Chem.* **1996**, *100* (10), 4064.
(21) Burel, L.; Mostafavi, M.; Murata, S.; Tachiya, M. *J. Phys. Chem. A* **1999**, *103* (30), 5882.

JP8004794